Aquatic Geochemistry **10:** 269–301, 2004.

Stable Carbon and Nitrogen Isotopic Composition of Benthic and Pelagic Organic Matter in Lakes of the McMurdo Dry Valleys, Antarctica

JENNIFER LAWSON[1,*], PETER T. DORAN[1], FABIEN KENIG[1], DAVID J. DES MARAIS[2] and JOHN C. PRISCU[3]

[1]*Department of Earth and Environmental Sciences, University of Illinois at Chicago, Chicago, Illinois 60607-7059, USA;* [2]*NASA Ames Research Center, Moffett Field, California 94035, USA;* [3]*Department of Land Resources and Environmental Sciences, Montana State University at Bozeman, Bozeman, Montana 59717-3120, USA*

Abstract. The perennially ice-covered lakes in the McMurdo Dry Valleys, Antarctica, are part of the coldest and driest ecosystem on earth. To understand lacustrine carbon and nitrogen cycling in this end-member ecosystem, and to define paleolimnological proxies for ice-covered lakes, we measured the stable carbon and nitrogen isotopic composition of particulate organic matter (POM) and benthic organic matter (BOM) within the lakes of Taylor Valley. The $\delta^{13}C$ compositions of seasonally ice-free edges of the lakes (moats) are enriched relative to under-ice organic matter. Thus, the organic carbon isotopic composition of buried sediments may be a proxy for sample position within the lake. In the moats, $\delta^{13}C$ values are governed by limited CO_2 diffusion across benthic cyanobacterial cell membranes. During a high glacial melt (2001–2002) season, both $\delta^{13}C_{POM}$ and $\delta^{13}C_{BOM}$ in the moats were more depleted than during previous low melt years. We propose that this occurred in response to higher $[CO_2]_{(aq)}$ and/or reduced growth rates resulting from turbidity-induced light limitation. Though moats and under-ice environments are usually poorly connected, during the 2001–2002 season, the enrichment of the $\delta^{13}C_{POM}$ values at 6 m depth in the stream-proximal sites relative to deep-profile sites implies enhanced connectivity between these environments. The $\delta^{13}C$ compositions of BOM and POM profiles in Lake Hoare and Lake Fryxell indicate that these lakes are dominated by benthic productivity. In contrast, in Lake Bonney, the similarity of the $\delta^{13}C$ values of BOM and POM indicates the pelagic component dominance in the carbon cycle.

Key words: carbon stable isotope, nitrogen stable isotope, organic matter, limnology, Antarctica, dry valleys, Taylor Valley

1. Introduction

Stable isotopic carbon and nitrogen compositions of organic matter (OM) have been widely used to trace biogeochemical processes in lacustrine and marine environments (e.g., Hedges et al., 2001; Lehmann et al., 2002; Meyers

* Author for correspondence, E-mail: jlawso2@uic.edu

and Eadie, 1993; Quay et al., 1986). The isotopic compositions of particulate and sedimentary OM are useful in assessing their origins and studying carbon cycling in lake systems (e.g., Gu et al., 1996; Hecky et al., 1993; LaZerte, 1983; Ostrom et al., 1998; Quay et al., 1992). Besides the importance of knowing the origin of OM carbon and nitrogen to understand modern ecosystem structure and function, the isotopic signature of carbon and nitrogen accumulating in sediments can also provide powerful proxies for paleolimnological reconstruction (e.g., Harvey et al., 1995; Henrichs and Doyle, 1986; Macko and Ostrom, 1994; Meyers and Eadie, 1993; Meyers and Ishiwatari, 1993).

Antarctic lakes of the McMurdo Dry Valleys (MDVs) represent one of the coldest ecosystems on earth (Doran et al., 2002a; Fountain et al., 1999). In these extreme environments, the constraints imposed on carbon and nitrogen isotopic signatures of lake OM transformations by minimal stream input, closed lake basins, permanent lake ice-covers, and strong salinity stratification have not been thoroughly studied. The physical limnology of these ice-covered lakes are considerably different from well-studied mid- and low-latitude lakes (e.g., Brenner et al., 1999; McKenzie, 1980).

The distribution and isotopic composition of organic carbon and nitrogen in soils of the dry valleys have been investigated to characterize allochthonous inputs to the lakes and provenance of soil OM (Burkins et al., 2000; Fritsen et al., 2000). Studies of carbon and nitrogen isotopic chemistry of OM in the MDV lakes have predominantly focused on Lake Hoare (Bishop et al., 2001; Doran et al., 1998; Neumann et al., 1998; Wharton et al., 1993). In Lake Hoare, the carbon isotopic composition of microbial mats, sediments, and dissolved inorganic carbon (DIC) have indicated that diffusion limitation of CO_2 across cell membranes is a major control of the isotopic composition of benthic organic matter (BOM), while in deeper zones, there is preferential uptake of ^{12}C due to supersaturation of $[CO_2]_{(aq)}$, approaching full expression of the ribulose-1,5-bisphosphate carboxylase (RUBISCO) enzyme (Doran et al., 1998).

In this paper we characterize the $\delta^{13}C$ and $\delta^{15}N$ of various OM pools in four MDV lakes, as well as associated $\delta^{13}C$ of DIC in the lake water to better understand OM transformations in these systems. These results refine our knowledge of carbon and nitrogen flow in these lake ecosystems and provide a calibrated sediment signature for future paleoenvironmental work.

2. Environmental Setting and Character of Taylor Valley Lakes

Taylor Valley (TV) is one of the MDVs of east Antarctica (Figure 1). In this polar desert, valley bottom mean annual precipitation is less than 10 cm and mean annual temperatures range from −14.8 to −30 °C (Doran et al., 2002b).

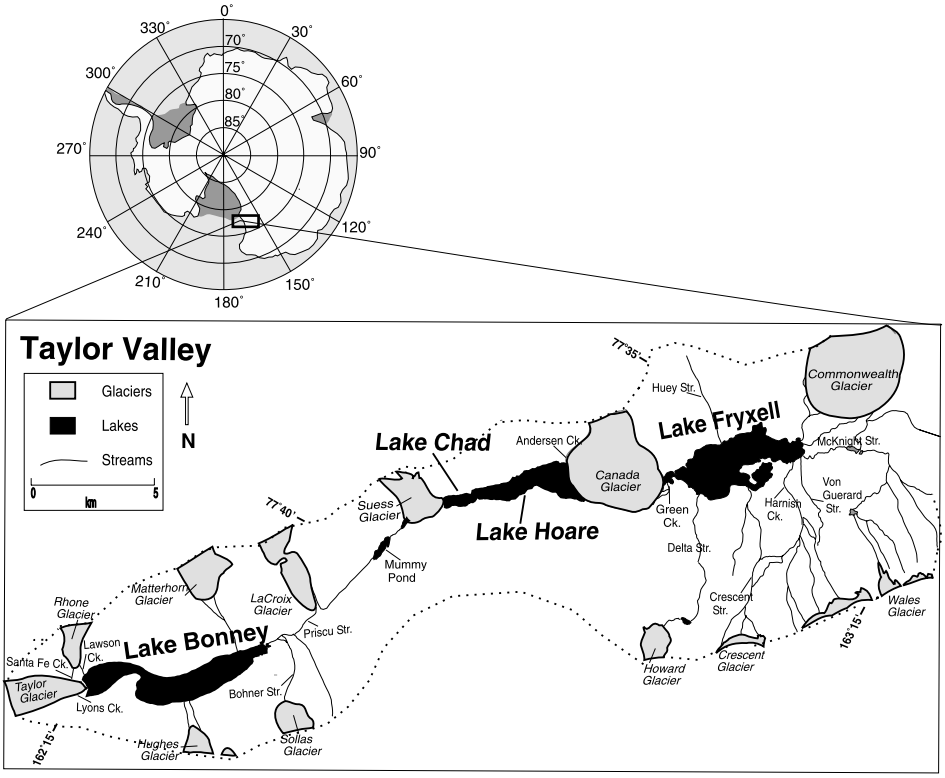

Figure 1. Map of Taylor Valley showing all major landscape units (http://huey.colorado.edu).

Despite these extremes, liquid water is present throughout the year in ice-covered lakes and during the summer months, glacial melt water feeds ephemeral streams that supply the lakes.

We focus on four main lakes in TV: Lake Fryxell, Lake Hoare, East Lake Bonney (ELB), and West Lake Bonney (WLB). Distinguishing physical and chemical parameters of each lake are presented in Table I and Figures 2–4. The two lobes of Lake Bonney are dealt with separately since they are geochemically and biologically distinct, being only connected though their surface waters at a shallow (12 m) channel (Spigel and Priscu, 1998). These lakes have no surface outflows, and are permanently covered by 3–6 m of ice. The water columns maintain their stratification year-round, a result of the wind-shielding effect of the ice-cover, low advective stream flow, and strong chemical gradients (Spigel and Priscu, 1998).

During most austral summers, edges of the lakes melt out creating ice-free moats that can be up to 3% of the lake surface area (Wharton et al., 1986) and are larger near stream mouths (Miller and Aiken, 1996), and smaller in areas of the lakes where the lake bed drops off steeply from the shore (e.g.,

Table I. Physical and chemical characteristics of Taylor Valley Lakes

	Lake Fryxell	Lake Hoare	East Lake Bonney	West Lake Bonney
Maximum depth (m)	20	34	40	40
Maximum length (km)	5.8	4.2	4.8	2.6
Maximum width (km)	2.1	1	0.9	0.9
Surface area (SA) ($m^2 \times 10^6$)	7.08	2.9	3.32	0.99
Volume (V) ($m^3 \times 10^6$)	53.4	24.2	72.4	17.4
SA:V (m^{-1})	0.13	0.12	0.05	0.06
Average ice thickness (m)	3.3–4.5	3.1–5.5	3–4.5	2.8–4.5
$CO_{2(aq)}$ equilibrium depth[a]	0 m[b]	10 m	10 m	10 m[c]
Depth of PPR max	5 and 9 m	6 m	12 m	13 m

[a]Below this depth water is saturated in CO_2. Water below chemoclines is highly supersaturated in CO_2 and shows no seasonal variation, except in Lake Hoare. Data from Neumann et al. (2001).
[b]All depths in Lake Fryxell are saturated with respect to CO_2.
[c]Equilibrium depth shifts to 6 m later in summer season.
Note: data from http://huey.colorado.edu.

much of WLB and ELB). Although there is hydrologic exchange between the moat and under-ice environments, as evidenced by their common level in the late summer, exchange must be limited, as reflected by various geochemical signatures. For example, isolation of the lakes from the atmosphere is indicated by very old ages (low ^{14}C abundance) of DIC (Doran et al., 1999), and supersaturation of trapped dissolved gases which accumulate through physical and biological processes (Andersen et al., 1998; Neumann et al., 1998; Priscu et al., 1998; Wharton et al., 1986, 1987). Yet, in deep waters of Lakes Fryxell and Hoare, some exchange with the atmosphere is indicated by presence of anthropogenic ^3H (Miller and Aiken, 1996) and chlorofluorocarbon compounds (Tyler et al., 1998).

Local glaciers supply meltwater to the lakes, either directly or via streams, during an 8–12 week period during the austral summer. Meltwater to Lake Fryxell basin is stream dominated with a smaller direct glacier meltwater component (McKnight and Andrews, 1993a). Lake Hoare receives most meltwaters from direct glacial melt off Canada Glacier or from Andersen Creek, whose source is Canada Glacier (McKnight and Andrews, 1993b). A smaller lake to the west, Lake Chad, also drains into Lake Hoare during high lake stands (McKnight and Andrews, 1993b). WLB receives its freshwater directly from Taylor Glacier and its alpine streams, while ELB, the only lake not directly in contact with a glacier, receives most of its water from WLB through the Bonney narrows and from Priscu Stream (Spigel and Priscu, 1998).

All the lakes have fresh surface waters and saline bottom waters, the exception being Lake Hoare, which is fresh throughout its water column

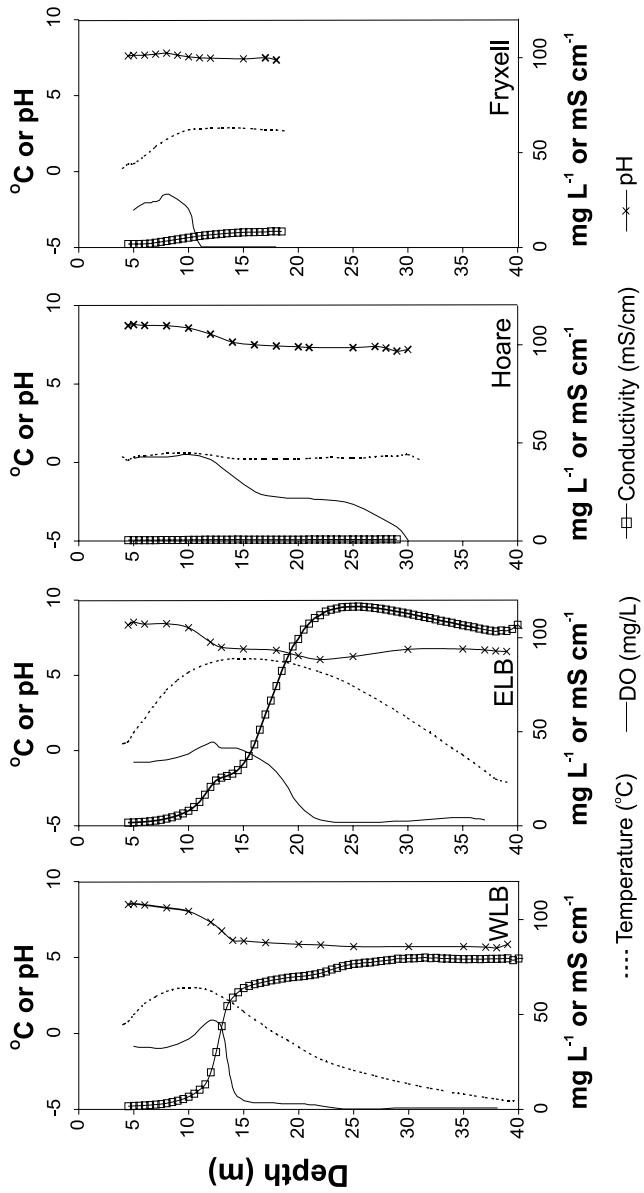

Figure 2. Temperature, conductivity, pH and dissolved oxygen profiles. The DO, pH (pH scale) and temperature profiles (°C) are mean values from the McM LTER data set (http://huey.colorado.edu) from 1993 to 2000. Conductivity data (mS/cm) for the same time-series are provided by J. C. Priscu, unpublished data.

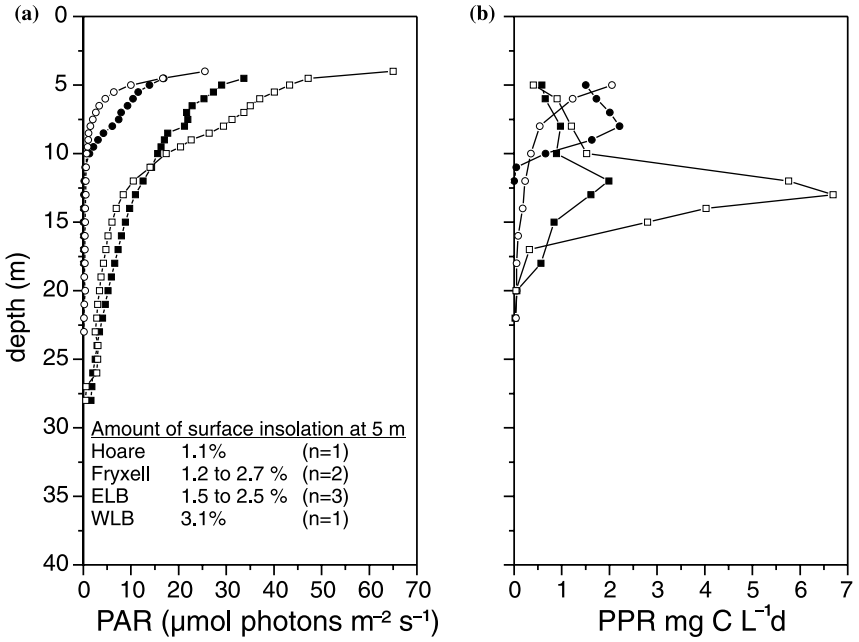

Figure 3. (a) Photosynthetically active radiation (PAR) for Taylor Valley lakes. Lines for each of lake represent the average of the three profiles with the highest average radiation in a record of summer PAR from 1993 to 2000. All profiles meeting these criteria fell in December. The amount of ambient surface light penetrating the ice-cover to reach 5 m depth in the water column is shown in the box. Each profile chosen for this comparison did not have a corresponding surface PAR measurement resulting in the different sample sizes in the box. (b) Primary productivities (PPR) for Taylor Valley lakes. Lines for each lake represent the 1993–2000 averages during the month of December. Figure 3a and b show ELB (closed square), WLB (open square), Lake Fryxell (closed circle), and Lake Hoare (open circle).

(Spigel and Priscu, 1998). ELB and WLB have hypersaline bottom waters, and Lake Fryxell's bottom waters below 9.5 m are brackish (Figure 2). The late Quaternary glacial history of TV has played a critical role in shaping the salinity profile of the lakes. About 12.7–23.8 kyr BP the valley was inundated by Glacial Lake Washburn (Hall et al., 2000; Hendy, 2000a), which was formed by damming of the eastern end of the valley by the Ross Ice Shelf. Washburn lake levels fluctuated significantly following the last glacial maximum, and ultimately drained following the Ross Ice Shelf retreat approximately 8.3 kyr BP (Hall and Denton, 2000a, b). Lake levels in the dry valleys have continuously changed being mostly at or below current levels since about 8 kyr BP (Doran et al., 2004). Of particular note is a severe cold and dry period about 1.2 kyr BP when Lakes Bonney and Fryxell were drawn down to small brine ponds, before being refilled with fresh glacial melt, contributing to the strong salinity gradient we see today (Lyons et al., 1998).

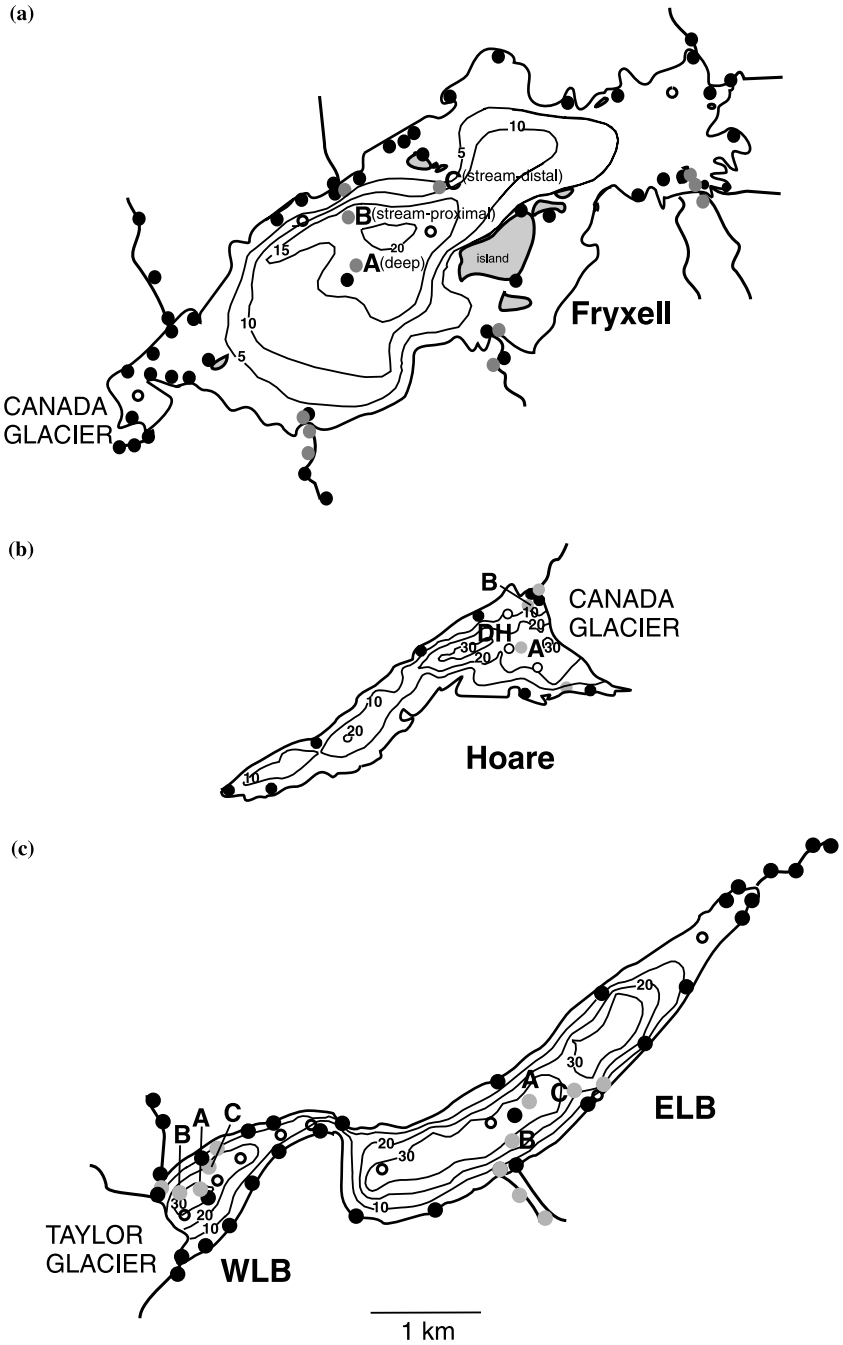

Figure 4. Sample locations and bathymetry of each lake. Black, grey, and open dots represent samples collected in 1999–2000, 2000–2001, and 2001–2002 field seasons, respectively. The grey dots located in the center basins of Lake Fryxell, Lake Hoare, ELB, and WLB, represent the POM profile sampling localities and are labeled A, B, and C. The significance of this nomenclature is made clear in Figure 5.

The difference in salinity between these two lakes is believed to be related to differential frequency of desiccation/salt deflation events (Lyons et al., 1999, 1998); deflation presumably happened less frequently in Lake Bonney. Lake Hoare is believed to have dried up completely during the 1.2 kyr BP drawdown, the salts deflated, and freshwater reintroduced to the basin creating the relatively fresh water column of today. Loss of ice-cover and wind-driven mixing of TV lakes has almost certainly contributed to their current physiochemical state, but presently, little is known about the ice-cover history.

When perennial ice-cover is present, sediments can be blown across the lake cover or trapped on the ice surface. During the summer, trapped sediments get warmed by the sun and melt into the ice. The dynamics of sediment movement within the ice-cover have been thoroughly described by several authors (Adams et al., 1998; Andersen et al., 1993; Hendy, 2000b; McKay et al., 1985; Priscu, 1998) and will not be repeated here. As such, differences in the sediment load of the ice-covers, in conjunction with ice thickness and bubble density, are likely responsible for the variable light regimes in the lake water columns (Figure 3a). Lake Bonney has thinner and cleaner ice-covers, while Lake Hoare and Lake Fryxell have thicker ice-covers (Doran et al., 2002b) containing a higher sediment concentration (Konley, 2002).

Benthic microbial mats in Taylor Valley lake moats are primarily composed of cyanobacteria (Hawes and Schwarz, 1999; Wharton et al, 1983). These mats are generally thinner than their under-ice counterparts and follow the contours of the sediment and rocks in the moats (Hawes and Schwarz, 1999). Deeper under-ice microbial mats consist primarily of cyanobacteria along with several species of pennate diatoms and heterotrophic bacteria, although their macromorphology differs as controlled by the unique physiochemical parameters in each lake (Wharton et al., 1983). Of note, is the lack of photoautotrophic mat growth below ~20 m in Lake Bonney (Priscu, 1992; Wharton, 1983).

The TV lakes' current light regime and water column stratification constrain the distribution of photoautotrophy. For instance, in the deepest part of ELB, a nutrient rich pool of high salinity water was formed during a past evaporation event and subsequently covered by nutrient deficient water (Priscu, 1995; Priscu et al., 1999). Because the lakes are permanently ice-covered and strongly density stratified, the deep nutrients are transported slowly upwards by molecular diffusion. Primary productivity (PPR) near the surface of the lakes is nutrient-limited, and therefore productivity maxima are found lower in the water column where light levels decrease, but nutrients are more abundant (Priscu, 1995; Priscu et al., 1999). One exception is Lake Hoare, where PPR is light limited and nutrient concentrations remain relatively unchanged with depth (Figure 3b).

The PPR data presented in Figure 3b were obtained from pelagic profiles in the center of the lakes. However, whole-lake productivity, inclusive of benthic contribution, is only known for Lake Hoare (Moorhead and Hawes, unpublished data). In steep-sided lakes like Lake Bonney, the benthic contribution to whole-lake PPR is expected to be very small. The opposite extreme is Lake Fryxell where the high area/volume ratio and relatively shallow depth (Table I) suggest that the benthic PPR may dominate whole-lake PPR. Hawes and Schwarz (1999) have estimated *in situ* benthic production (December 1996) in Lake Hoare moats as 140 mg C m^{-2} d^{-1} and ranges from 10 to 110 mg C m^{-2} d^{-1} under the ice. These rates of *in situ* benthic productivity are very high relative to those measured for pelagic communities. Priscu (1995) calculated daily integrated PPR as 7.5 mg C m^{-2} d^{-1}, making the pelagic component less than 10% of the whole-lake PPR in Lake Hoare.

3. Methods

3.1. FIELD METHODS

Water column and sedimentary OM were collected in each of the four TV lakes over three Antarctic summer field seasons (November January 1999–2002). The 1999–2000 season involved collecting sediment surface OM (microbial mat and/or sediment) along the long-axes of the lakes including associated water samples from immediately above the sediment/water interface (Figure 4). Extensive moat and stream sampling occurred throughout the 2000–2001 season. In comparison to the previous two field seasons, the 2001–2002 austral summer had widespread glacial melt and large moat development, estimated to be at least 3–4 times larger than in previous years. Lake levels rose approximately 1 m and there was a 5-fold increase in total stream flow of all TV gauged streams from 2000–2001 (1.2×10^6 m^3) to 2001–2002 (5.2×10^6 m^3) summers (P.T. Doran, unpublished data). We refer to the 2001–2002 season as the ''flood year'' and the previous two field seasons as ''non-flood years''. During the flood year, stream-proximal and stream-distal depth transects were sampled in each of the four lakes (Figure 5). Within these transects, we sampled POM at 5–8 (depending on lake depth) discrete water depths and BOM at lake bottom.

Ice-cover sediment was collected from the Lake Hoare ice surface in three locations (east, center, west), along the long axis of the lake. Benthic surface sediment samples were also collected by dredging from the ice surface or directly by SCUBA-equipped divers. In the deep waters of ELB, sediments were mostly halite crystals; therefore, sediments were scraped from the dredged crystals for analyses. All samples were immediately wrapped in precombusted aluminum foil, inserted into Whirl-pak bags and frozen at −20 °C.

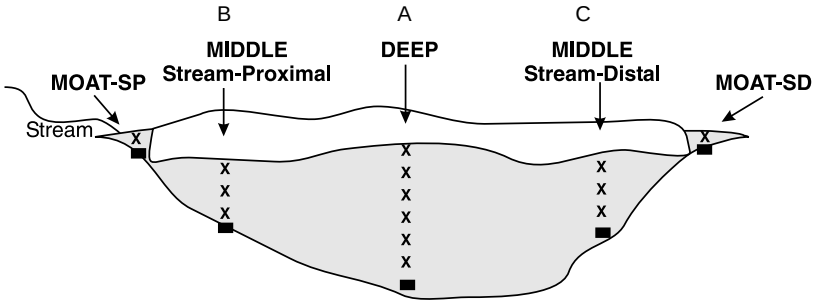

Figure 5. Lake basin cross-section showing the particulate and benthic OM sampling scheme during 2001–2002 season. X's represent POM sample localities, while black squares indicate BOM samples. Deep samples are labeled A, while the stream-distal and stream-proximal middle samples are labeled B and C, respectively. Locations are also shown in plane view in Figure 4.

Ten sediment traps were deployed in November 2000 on the sediment surface at 8 m depth in Lake Hoare (see location on Figure 4b) and retrieved 2 years later. These traps were 1 L amber Nalgene bottles with affixed legs. The bottles were poisoned with 5 mg L^{-1} solutions of benzalkonium chloride and sodium chloride (Acros Organic). Large Mark 78H-21 PARFLUX time series sediment traps (McLane Research) were deployed at 35 m in the deep basin centers of Lake Bonney in December of 2000 and recovered one year later. These traps were also poisoned with benzalkonium chloride (<5 mg L^{-1}).

At each sampling depth, 3 L of water was collected using Kemmerer bottles. Water was slowly transferred from a release valve at the end of the Kemmerer bottle into deionized water rinsed 1 L high density polyethylene (HDPE) amber bottles, allowed to overflow, and then capped. In shallow moat regions, water was collected directly into the three submerged HDPE Nalgene bottles. In the field, DIC water samples were then filtered into precombusted glass serum bottles through precombusted 25 mm Whatman GF/F syringe filters, poisoned with benzalkonium chloride, and sealed with Teflon-faced septa.

3.2. LABORATORY METHODS

Sediment surface samples were dried at 60 °C for 48 h and sieved through 2 mm mesh sieves. McLane sediment trap samples were sieved into three fractions <63 μm, 63–250 μm, and >250 μm. Carbon and nitrogen isotope analyses were conducted on the Thermo Finnigan Delta Plus XL Mass Spectrometer interfaced with a CE Instruments NC2500 Elemental Analyzer with an A200 autosampler at the Environmental Isotope Geochemistry Lab, University of Illinois at Chicago. All stable isotope signatures are reported as per mil relative to VPDB and air for carbon and nitrogen, respectively.

Lacustrine BOM samples were tested for sample heterogeneity. Because grain sizes in moat samples are coarser than in deep samples, two different moat samples and a deep lake basin sample were used to test for differences in precision of isotopic data between samples with very different granulometry. The standard deviation for sandy moat samples ($n = 18$) was 0.4‰ for $\delta^{15}N$ and 1.1‰ for $\delta^{13}C$ ($n = 19$), while in a microbial mat dominated (no sand particles) moat sample, the standard deviation was 0.6‰ for $\delta^{15}N$ ($n = 18$) and 0.9‰ for $\delta^{13}C$ ($n = 20$). The standard deviation for deep BOM was 0.5‰ for $\delta^{15}N$ ($n = 20$), and 0.6‰ for $\delta^{13}C$ ($n = 20$). The instrument analytical precision for $\delta^{13}C$ is 0.1‰ and $\delta^{15}N$ is 0.2‰.

For stable carbon isotopic analyses, POM was filtered from an aliquot (700—2700 ml) of lake water sample onto precombusted 47 mm Whatman GF/F glass fiber filters and then dried at 60 °C for 24 h. These filters were subsampled by punching 9 mm diameter disks that were subsequently cut and placed inside 5 × 9 mm silver capsules, acidified with sulfurous acid, and dried again at 60 °C prior to analyses. Internal POM standards were developed to test for homogeneity and accuracy in field sampling and lab techniques. We analyzed several duplicates and portions of the same filter sample. These sampling errors fell within the analytical error of the mass spectrometer.

DIC water samples for $\delta^{13}C$ analyses were cryogenically separated on a vacuum extraction line and analyzed at the Stable Isotope Laboratory, Ann Arbor Michigan, on a Finnigan MAT Delta S, with an analytical precision of 0.11‰.

Microbial species identifications were conducted at Desert Research Institute, Reno, Nevada, with a combination of light and epifluorescent microscopy (Olympus BX 60).

3.3. $\delta^{13}C$ OF SEDIMENT TRAP ORGANIC MATTER

Weighted average carbon isotopic signatures ($\delta^{13}C_{OM}$) were calculated for ELB and WLB sediment trap samples using Equation (1).

$$\delta^{13}C_{OM} = \frac{\delta^{13}C_{<63}(C_{<63}) + \delta^{13}C_{63-250}(C_{63-250}) + \delta^{13}C_{>250}(C_{>250})}{(C_{<63} + C_{63-250} + C_{>250})}. \quad (1)$$

Subscripts represent the grain size fractions (μm) of the sediments and weights of carbon (values inside the parentheses) are in mg. We calculated averaged weights by averaging the carbon composition for each individual grain size fraction per lake and the associated isotopic composition for the grain size. This method was used to eliminate any bias from using too few samples, as only a total of five samples out of a possible 29 had all three grain sizes recovered and analyzed for their $\delta^{13}C$ values. This also assumes that the average isotopic compositions are representative of those particular grain size

fractions. This assumption is valid as each grain size fraction is significantly distinct from the others. The weighted carbon isotopic average for ELB sediment traps was −13.9 ± 0.7‰, while that of WLB was −30.5 ± 0.5‰. To check that our isotopic composition averaging of the grain size fractions was valid, we calculated weighted $\delta^{13}C$ for samples which we have all three grain size fractions (Table II) and averaged those results. The ELB and WLB weighted averages are −15.6 ± 2.9‰ (n = 2), −30.75 ± 0.6‰ (n = 3), respectively.

4. Results

4.1. INTER-LAKE COMPARISONS OF ORGANIC MATTER

We have expanded on the $\delta^{13}C$ and $\delta^{15}N$ ranges of lacustrine OM put forth by Wharton et al. (1993) for Lake Hoare and Burkins et al. (2000) for the MDVs (Figure 6a). Our results show that moat BOM can be clearly distinguished from the more ^{13}C depleted and occasionally more ^{15}N enriched BOM of permanently ice-covered parts of the lakes (Figure 6b). Moat $\delta^{13}C_{POM}$ is also more enriched (−11.2 to −29.4‰) compared to the deep lake samples (−25.2 to −38.9‰) (Figure 6c). There is a range of ~14‰ for both moat $\delta^{15}N_{POM}$ (−12.3 to 2.9‰) and deep $\delta^{15}N_{POM}$ (−7.4 to 6.1‰). It is noteworthy that although moat BOM samples were collected between 0–2 m, there was no isotopic change with depth in the moats (Figure 7).

The majority of our data for $\delta^{15}N$ of both BOM and POM fall between 5‰ and −5‰. The $\delta^{15}N$ of aquatic OM is generally between 20‰ and −17‰ (e.g., Bernasconi et al., 1997; Hamilton and Lewis, 1992; Kendall et al., 2001). When combining all under-ice $\delta^{15}N_{POM}$ from all lakes, there is a weak ($r^2 = 0.28$) but significant ($P < 0.0001$) increase with depth. Furthermore, t-tests show that deep $\delta^{15}N_{BOM}$ (mean = −1.1‰) is significantly ($P = 0.005$) different than all other shallower $\delta^{15}N_{BOM}$ (mean = −2.6‰), and deep $\delta^{15}N_{POM}$ (mean = −0.8‰) is significantly ($P = 0.02$) different than all other shallower $\delta^{15}N_{POM}$ (mean = −1.9‰)

The BOM of the moats is mainly microbial mat material with a variety of cyanobacterial species, dominantly *Phormidium*, *Oscillatoria*, *Plectonema*, and *Nostoc* (Table III), as also described by Wharton et al. (1983) and Hawes and Schwarz (1999). Samples described in the field as green (G), correspond to *Oscillatoria* or *Nostoc* dominated mats, while red (R) mats are formed by *Plectonema*. Heterotrophic bacteria have yet to be fully characterized but initial estimates from Lake Fryxell suggest a diverse bacterial assemblage is present along with the cyanobacteria, as shown by Karr et al. (2003). There is no distinct pattern relating cyanobacterial species composition and stable isotopic signatures of both carbon and nitrogen (Table III). For example, at

Table II. Stable carbon isotope signatures and carbon weights of McLane sediment trap samples

East Lake Bonney							West Lake Bonney						
Sample ID[a]	$\delta^{13}C$ (< 63 μm)	Total C (mg) (< 63 μm)	$\delta^{13}C$ (63–250 μm)	Total C (mg) (63–250 μm)	$\delta^{13}C$ > 250 μm	Total C (mg) > 250 μm	Sample ID[a]	$\delta^{13}C$ (< 63 μm)	Total C (mg) (< 63 μm)	$\delta^{13}C$ (63–250 μm)	Total C (mg) (63–250 μm)	$\delta^{13}C$ > 250 μm	Total C (mg) > 250 μm
ELB 1		0.18	−19.57	2.70	−13.38	25.11	WLB 1	−31.29	174.09	−26.73	0.62	−18.35	2.33
ELB 2		0.32	−20.89	7.81	−13.63	15.48	WLB 2	−31.52	106.12		0.02	−17.14	1.21
ELB 3	−27.58	1.15	−19.94	35.85	−12.28	100.49	WLB 3	−30.50	119.07	−23.79	0.43	−13.78	3.12
ELB 4	−28.28	0.68	−19.95	14.44	−11.91	70.04	WLB 4	−30.58	117.11	−21.92	0.24	−12.30	1.27
ELB 5		0.86	−19.29	13.98	−11.45	53.44	WLB 5	−30.03	28.71		0.15	−13.64	0.87
ELB 6		0.25	−19.65	6.26	−11.73	41.32	WLB 6	−30.22	35.14	−25.40	0.25		0.40
ELB 7		0.09	−22.32	2.18	−13.23	16.74	WLB 7	−30.74	17.10		0.18		0.08
ELB 8		0.30	−21.22	3.07	−14.34	10.72	WLB 8	−30.85	28.97		0.33		0.12
ELB 9		0.34	−24.15	1.30	−14.61	11.13	WLB 9	−30.96	7.28		0.06	−12.31	0.15
ELB 10		0.22	−23.99	5.33	−14.75	29.49	WLB 10	−32.69	7.95		0.15		0.31
ELB 11		2.45	−22.13	1.33	−16.59	18.77	WLB 11	−31.89	13.34		0.11		0.03
ELB 12		0.08	−24.83	0.68	−15.14	3.39	WLB 12	−31.15	4.65		0.02		0.01
ELB 13		0.08		0.24	−20.82	1.36	WLB 13	−31.19	3.25		0.19		
ELB 14		0.18			−10.51	1.56	WLB 14	−31.57	3.78				
							WLB 15		2.29				
Mean	−27.93	0.54	−21.50	28.50	−13.88	7.32	Mean	−31.08	44.59	−24.46	0.21	−14.59	0.83
Std. dev.	0.50	0.66	1.97	28.85	2.59	9.78	Std. dev.	0.70	55.50	2.08	0.17	2.55	1.0
Number	2	14	12	14	14	14	Number	14	15	4	13	6	12
Total		7.18		95.17		399.04			668.85		2.75		9.90

[a]Each sediment trap sample records fallout at 35 m depth in both ELB and WLB for approximately 16–18 days.

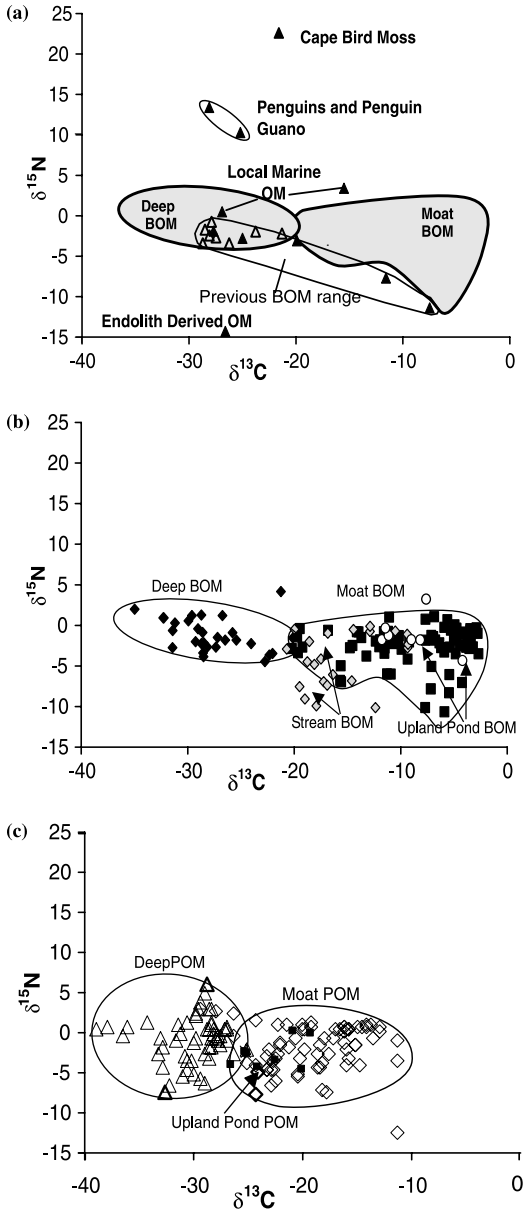

Figure 6. (a) The shaded ellipsoidal shapes indicate the new BOM ranges for the moat and deep lake environments. Also included are published stable isotope data from Burkins et al. (2000) (solid triangles) and Wharton et al. (1993) (open triangles) of various OM types from the MDVs, encompassed by a thinly outlined ellipse denoting the previous BOM range. (b) The new lacustrine range of OM is divided between deep BOM and moat BOM. Also shown are the $\delta^{13}C$ and $\delta^{15}N$ regions for streams and upland pond BOM from Taylor Valley. (c) Moat POM and Deep POM ranges are shown for Taylor Valley lakes.

the site Fryxell-00-21, red and green samples were collected, as there were two coexisting microbial communities with different colors apparent at the time of sampling. The carbon and nitrogen isotopic composition of these samples are indistinguishable (Table IV), as they are within one standard deviation established for heterogeneous moat samples (0.9–1.1‰ for $\delta^{13}C$ and 0.4‰–0.7‰ for $\delta^{15}N$).

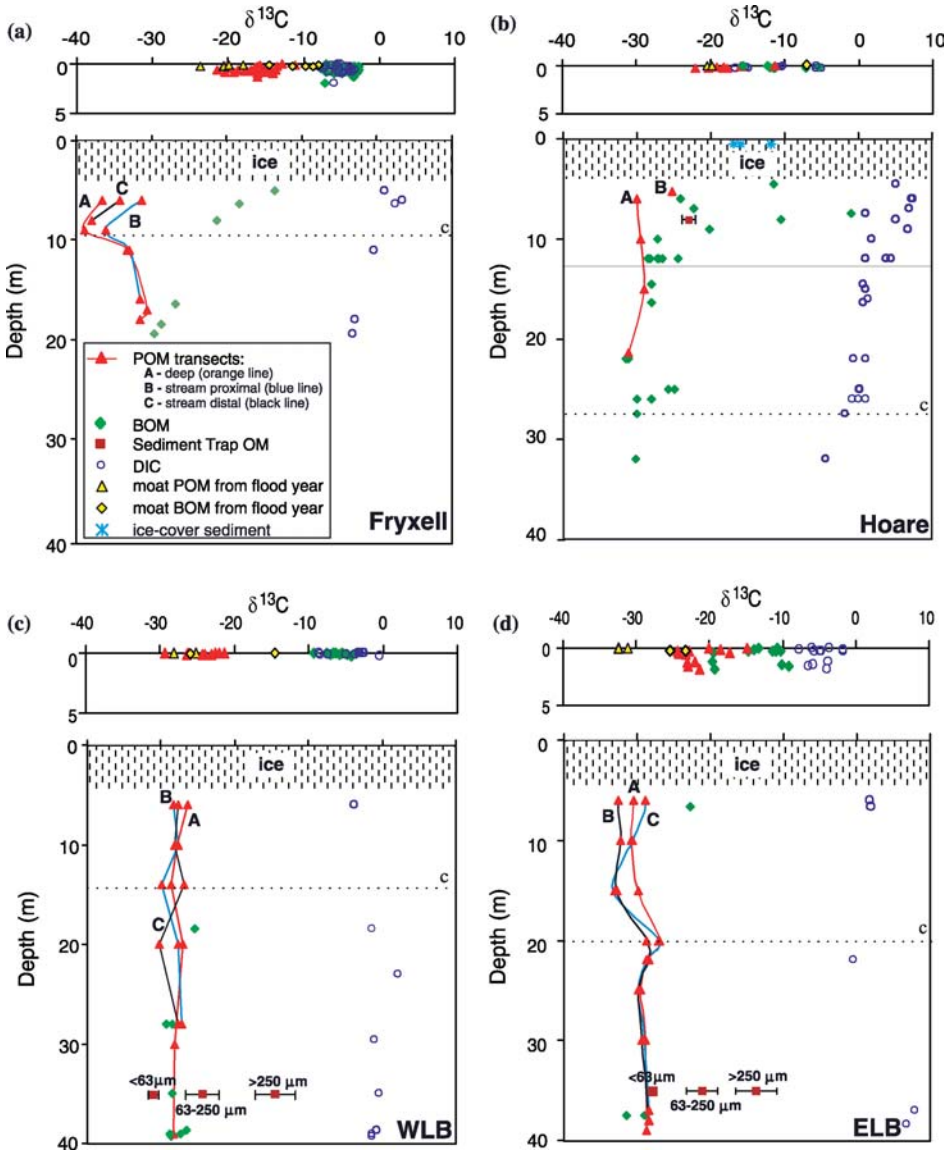

Figure 7. All plots (a, b, c, d) show $\delta^{13}C$ values for BOM (diamonds), POM (triangles), and DIC (open circles). Moat samples 0–5 m are plotted separately from those samples below the ice-cover. The dotted line indicates the presence of the chemocline (c). Only POM profiles (A, B, C,) are connected with lines at 6 m and below, as each profile represents samples taken from the same water column. The yellow symbols represent moat samples collected during the flood year. (a) Lake Fryxell stable carbon isotope signatures with depth. (b) Lake Hoare stable carbon stable isotope signatures with depth. The black line at 13 m denotes the CO_2 saturation line, indicating saturation at depth. The brown square represents the average $\delta^{13}C$ value of sediment traps at 8 m ($n = 10$). Three surface ice-cover sediment (blue stars) samples are plotted in the depth diagram with ice-cover. (c) WLB stable carbon stable isotope signatures with depth. The brown squares represent the average $\delta^{13}C$ values of three sieved fractions from benthic sediment traps at 35 m in the center of WLB. (d) ELB stable carbon stable isotope signatures with depth. The brown squares represent the average $\delta^{13}C$ values of three sieved fractions from benthic sediment traps at 35 m in the center of ELB.

Table III. Cyanobacterial identification of moat microbial mats and associated isotope values. Moat mat species identification in order of abundance

Lake	Sample[a]	Depth (m)	Primary taxa	Secondary taxa	Tertiary taxa	$\delta^{13}C$	$\delta^{15}N$
Fryxell	00-03	0.6	Phormidium	Plectonema	Nostoc	−3.23	−0.5
Fryxell	00-21G	0.6	Oscillatoria	Plectonema	Nostoc	−4.46	−2.51
Fryxell	00-21R	0.6	Plectonema	Nostoc	Oscillatoria	−4.81	−1.81
Fryxell	00-22	0.2	Nostoc	Oscillatoria	Phormidium	−2.76	−0.99
Fryxell	00-29	0.1	Unicellular (Microcystis-like)	Nostoc	Plectonema	−6.86	1.05
Fryxell	00-30	0.2	Phormidium	Nostoc	Oscillatoria	−6.21	−2.75
Hoare	00-05	0.1	Phormidium			−11.5	−2.78
Hoare	00-08R	0.04	Plectonema	Oscillatoria	Unicellular Cyanobacteria (gleocapsa)	−15.59	−6.97
Hoare	00-09G	0.04	Nostoc	Plectonema	Phormidium	−12.34	−1.95
ELB	00-01	0.3	Phormidium			−10.24	−1.59
ELB	00-04	1.9	Plectonema	Nostoc	Oscillatoria	−19.22	−2.68
WLB	00-11	0.2	Unicellular (Microcystis-like)	Phormidium	Oscillatoria	−10.92	−6.01
WLB	00-06	0.2	Nostoc	Phormidium	Oscillatoria	−4.239	−7.06
WLB	00-10dry	0.0	Phormidium	Unicellular		−6.88	−2.18

[a]R, G, B, correspond to red, green, or black appearance of mat during field collection. Dry refers to mat that was desiccated on the shoreline when sampled.

Table IV. Microbial mat variability between species types and degrees of desiccation (age)

Sample ID[a]	Description	$\delta^{13}C$	$\delta^{15}N$
Fryxell-00-21G	Green moat mat	−4.46	−2.51
Fryxell-00-21R	Red moat mat	−4.81	−1.81
Chad-00-08 B	Black moat mat	−13.69	−1.51
Chad-00-08 G	Green moat mat	−14.12	−0.79
Fryxell-00-29	Moat mat	−6.86	1.05
Fryxell-0029 LO	Lift off mat from ice next to Fryxell-00-29	−5.74	−0.59
Fryxell-00-29 3	Dried lake shore mat from strand line (youngest) next to Fryxell-00-29.	−6.92	1.36
Fryxell-00-29 2	Dried lake shore mat from strand line centimeters above Fryxell-00-29 3.	−8.00	0.31
Fryxell-00-29-1.5	Dried lake shore mat from strand line centimeters above Fryxell-00-29 2.	−8.02	−1.27
Fryxell-00-29-1	Highest strand line (oldest) in series.	−11.00	−1.60

[a]R, G, B, correspond to red, green, or black appearance of mat during field collection.

4.1. LAKE FRYXELL

In the Lake Fryxell moat, BOM and DIC had virtually identical $\delta^{13}C$ signatures (−4.6 ± 1.4‰ and −5.2 ± 1.1‰, respectively), while POM is on average depleted in ^{13}C by ∼10‰ (Table V, Figure 7a). The moat $\delta^{13}C_{POM}$ ranges from −23.7 to −11.2‰ with a mean value of −16.6 ± 2.9‰ (n = 37).

Table V. Moat isotopic values—non-flood year (2000–2001)

	Fryxell	Hoare	ELB	WLB
$\delta^{13}C$ BOM				
Mean	−4.6	−10.9	−13.6	−6.1
Standard deviation	1.4	3.0	3.9	1.7
Range	5.0	10.2	10.4	5.8
Minimum value	−7.7	−15.6	−19.6	−9.4
Maximum value	−2.7	−5.4	−9.2	−3.6
Number	31	9	12	10
$\delta^{13}C$ DIC				
Mean	−5.2	−10.5	−4.4	−4.4
Standard deviation	1.1	4.4	1.6	2.7
Range	4.6	11.4	4.7	8.2
Minimum value	−7.9	−16.6	−6.4	−8.6
Maximum value	−3.3	−5.1	−1.7	−0.5
Number	32	9	11	11

Table V. Continued

	Fryxell	Hoare	ELB	WLB
$\delta^{13}C$ POM				
Mean	−16.6	−18.1	−21.2	−24.8
Standard deviation	2.9	3.0	3.0	2.7
Range	12.5	10.8	9.6	8.0
Minimum value	−23.7	−22.1	−24.3	−29.4
Maximum value	−11.2	−11.2	−14.8	−21.4
Number	37	11	12	10
^{13}C Fractionation (BOM-DIC)				
Mean	−0.6	0.4	9.6	1.6
Standard deviation	1.4	5.6	5.2	2.5
^{13}C Fractionation (POM-DIC)				
Mean	11.5	6.0	17.2	20.7
Standard deviation	3.7	7.2	2.7	4.7
$\delta^{15}N$ BOM				
Mean	−1.1	−3.4	−2.4	−4.0
Standard deviation	1.1	2.3	1.5	2.2
Range	4.6	5.7	5.6	6.5
Minimum value	−3.5	−7.0	−6.0	−8.3
Maximum value	1.1	−1.3	−0.4	−1.8
Number	31	9	12	10
$\delta^{15}N$ POM				
Mean	−0.4	−4.9	−3.8	−0.1
Standard deviation	1.4	3.7	2.6	2.7
Range	4.5	13.6	8.0	7.7
Minimum value	−3.3	−12.3	−7.6	−4.8
Maximum value	1.2	1.3	0.4	2.9
Number	32	10	9	10

Moat BOM samples from Lake Fryxell ranged from −11.5 to −8.0‰ and were more depleted in ^{13}C than the non-flood year moat BOM samples (Figure 7a). POM samples also show a more depleted $\delta^{13}C$ trend than average moat $\delta^{13}C_{POM}$ from the non-flood year (Figure 7a, Table V).

Below the ice-cover, both POM and BOM exhibit depleted $\delta^{13}C$ values, while the DIC initially becomes more enriched. At 6 m the stream-proximal $\delta^{13}C_{POM}$ is −31.3‰, while the deep transect 6 m $\delta^{13}C_{POM}$ is −36.5‰. Below the chemocline, DIC and BOM become ^{13}C depleted while POM becomes

more enriched with depth. At the lake bottom, $\delta^{13}C_{POM}$ and $\delta^{13}C_{BOM}$ values converge at around −30‰, and the DIC is significantly ^{13}C depleted relative to shallow water DIC.

4.2. LAKE HOARE

Even in the absence of a strong chemocline, Lake Hoare has a deep $\delta^{13}C_{BOM}$ and $\delta^{13}C_{DIC}$ profile similar to that of Lake Fryxell. The $\delta^{13}C_{BOM}$ is isotopically enriched in the moat and becomes more depleted with depth (Figure 7b). In Lake Fryxell, this BOM trend persists to the deepest part of the lake, while in Lake Hoare, the $\delta^{13}C_{BOM}$ depletion ends at around 20 m. The Lake Hoare moat is highly enriched in ^{13}C relative to the under-ice profile. The BOM and DIC in Lake Hoare moat is more ^{13}C depleted than in Lake Fryxell and the $\delta^{13}C_{BOM}$ more variable (Table V). Similar to Lake Fryxell, Lake Hoare moat $\delta^{13}C_{DIC}$ is indistinguishable from its $\delta^{13}C_{BOM}$. The mean $\delta^{13}C_{POM}$ in the moat (−18.1 ± 3.0‰, n = 11) is 8‰ more depleted in ^{13}C than moat DIC. Two of the three more depleted $\delta^{13}C_{POM}$ values represent flood year samples. The lone moat BOM sample from the flood year is similar to other years' moat $\delta^{13}C_{BOM}$.

From the surface of the ice-cover, three sediment samples yielded $\delta^{13}C$ values of −16.5‰, −15.7‰, and −11.0‰, representing ^{13}C enrichment in the ice-cover sediment. These ice-cover $\delta^{13}C$ values are similar to those of the moat $\delta^{13}C_{BOM}$.

The $\delta^{13}C_{POM}$ deep profile for Lake Hoare is relatively invariant with depth, with values averaging −29.9 ± 0.9‰. Lake Hoare lacks other POM transects, but a single sample, collected from a very shallow (5.5 m) stream-proximal locality, is 6‰ enriched in ^{13}C relative to deep water POM transect (Figure 7b).

The ten sediment trap samples at 8 m had a mean $\delta^{13}C$ value of −23.1 ± 0.6‰. This value is similar to BOM isotopic signatures at this depth, but approximately 5‰ enriched in ^{13}C compared to POM at the same depth (Figure 7b).

4.3. WEST LAKE BONNEY

The WLB moat $\delta^{13}C_{BOM}$ (−6.1 ± 1.7‰; n = 10) and $\delta^{13}C_{DIC}$ (−4.4 ± 2.7‰; n = 11) signatures resemble those of Lake Fryxell. Moat $\delta^{13}C_{POM}$ range from −21.4 to −29.4‰, being more depleted in ^{13}C than in the other TV lakes. The flood year moat POM samples are similar to corresponding POM transects (stream-distal or proximal) below the ice-cover, and are more depleted than the average $\delta^{13}C_{POM}$ from the non-flood year (Figure 7c). Moat BOM samples from the flood year are approximately 6 and 16‰ more depleted in ^{13}C than moat BOM from the previous year.

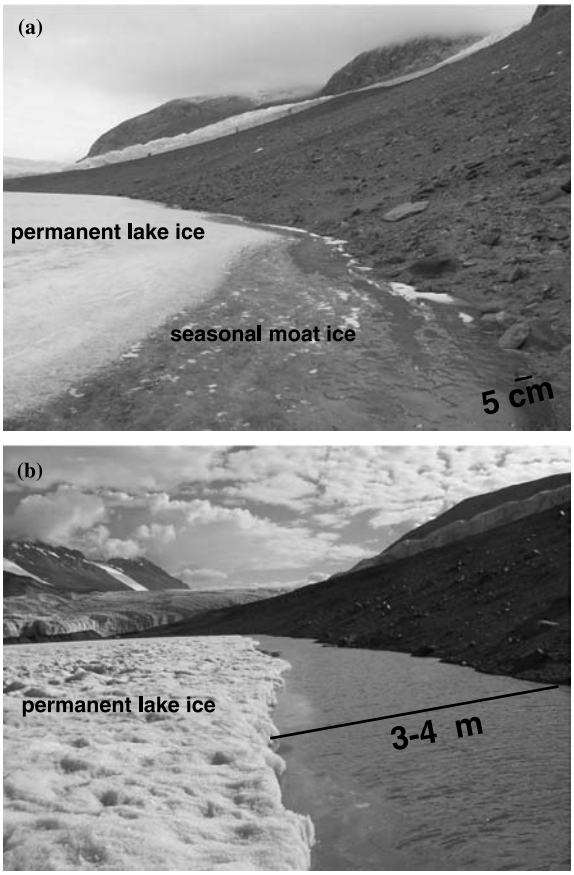

Figure 8. Photos of the moat area on the north side of West Lake Bonney. Photo (a) was taken January 11, 2001. Photo (b) was taken January 18, 2002 (flood year). The black line denotes open moat water showing the change in the size of moat development between the non-flood (2000–2001) and flood (2001–2002) years.

Water column profiles under the ice-cover in WLB show that $\delta^{13}C_{DIC}$ and $\delta^{13}C_{POM}$, as well as $\delta^{13}C_{BOM}$ are virtually identical and invariant with depth (Figure 7c). The distinct WLB chemocline at 14 m depth has little impact on the $\delta^{13}C$ signatures. All POM transects were collected within two consecutive days.

Isotopic signatures of the sediment trap samples in WLB were grain-size dependent (Figure 7c, Table VI). The largest grain size fraction (>250 μm) is the most enriched in ^{13}C ($-14.6 \pm 2.6‰$, $n = 6$), while the finest grain size (<63 μm), is the most depleted ($-31.1 \pm 0.7‰$, $n = 14$; Table VI). The >250 μm fraction has $\delta^{13}C$ values falling within the range of moat BOM values. The fine grain size fraction $\delta^{13}C$ values are comparable to the $\delta^{13}C_{POM}$ and the $\delta^{13}C_{BOM}$ below the ice-cover.

4.4. EAST LAKE BONNEY

The ELB moat differs from other TV lakes, in that $\delta^{13}C_{BOM}$ values (−19.6 to −9.2‰) do not overlap with $\delta^{13}C_{DIC}$ values (−6.4 to −1.7‰), which are approximately 9‰ more enriched in ^{13}C, on average (Figure 7d). The mean moat $\delta^{13}C_{BOM}$ is the most depleted of all TV lakes (−13.6 ± 3.9‰; n = 12), while moat DIC is −4.4 ± 1.6‰ (n = 11; Table V). The moat BOM is ~7.5‰ enriched in ^{13}C relative to moat POM (−21.2 ± 3.0‰; n = 12; Table V). The two most depleted $\delta^{13}C_{BOM}$ (−23.0 and −26.7‰) and $\delta^{13}C_{POM}$ values (−32.4 and −31.1‰) in the ELB were sampled during the flood season.

Under the ELB ice-cover, there is a large difference in $\delta^{13}C$ values between DIC and BOM that increases with depth as the BOM becomes isotopically more depleted. The deep BOM at 38 m depth, yield carbon isotopic values of −29 to −32‰. BOM profiles do not encompass all depths, as the steep bathymetry in ELB makes mid-depth sampling exceptionally difficult.

Besides this enrichment in ^{13}C of the stream-proximal 6 m location, the three POM profiles (collected within 3 days of each other) in ELB do not show any other systematic variation due to sample locality (e.g., steam-proximal vs. distal) at depth. $\delta^{13}C_{POM}$ in the upper water column (6–15 m) averages ~−32‰, while $\delta^{13}C_{POM}$ at the ELB chemocline is relatively enriched to ~−27‰. Below the chemocline, $\delta^{13}C_{POM}$ averages ~−29‰. This trend in the $\delta^{13}C_{POM}$ profile at ELB contrasts with that observed at the chemocline of Lake Fryxell (Figure 7a). At the deepest portion of ELB the $\delta^{13}C_{POM}$ and $\delta^{13}C_{BOM}$ converge, while the DIC becomes more enriched in ^{13}C.

The mean $\delta^{13}C_{BOM}$ of the sediment trap size fractions have a similar range to those of WLB (Figure 7c, and d, Table II). However, the < 63 μm fraction for ELB ($\delta^{13}C_{BOM} = -27.9 \pm 0.5$‰) is significantly more enriched (3‰) than for WLB ($\delta^{13}C_{BOM} = -31.1 \pm 0.7$‰).

5. Discussion

There is a characteristic $\delta^{13}C$ range for deep BOM (−20.1 to −35.0‰) and moat BOM (−2.7 to −20.2‰). This distinction is also observed in $\delta^{13}C_{POM}$ (Figure 7c), except in WLB (Figure 7c, Table IV). In contrast, the $\delta^{15}N$ signatures for lacustrine OM in the MDVs do not seem to be a very useful parameter to distinguish OM provenance in the lakes. The aquatic $\delta^{15}N$ signatures fall within a relatively narrow range of $\delta^{15}N$ as compared to OM from other MDV terrestrial environments (Figure 6a). However, a few observations can be made. First, the $\delta^{15}N$ signatures of deep BOM exhibit less variation than all other OM sources. Second, deep lake OM seems to be isotopically depleted with respect to $\delta^{15}N$ than shallow OM. The $\delta^{15}N$ of aquatic OM is controlled by the $\delta^{15}N$ of utilized dissolved inorganic nitrogen (DIN) and fractionations associated with processes that alter the nitrogen

composition of nitrate or ammonium in streams and lakes. Therefore, fractionation of $\delta^{15}N$ from its source must be relatively small in our samples. This also means that DIN sources must be minor and/or growth rates high, for such fractionation effects. These processes are inherently not associated with sample position in the lake.

5.1. STABLE ISOTOPE SIGNATURES IN THE MOATS

There is no obvious relationship between cyanobacterial composition and the stable carbon isotopic signature of moat mats in our data. Based on this observation, environmental parameters, such as CO_2 diffusion across cell membranes ice-cover extent, and number of sunlight hours, must be the major controls on carbon fractionation between DIC and BOM in the TV lakes. Mat forming cyanobacteria fix carbon via the C-3 (Calvin-Benson) pathway (Fuchs and Stupperich, 1985), which discriminate against ^{13}C as a result of RUBISCO activity (O'Leary, 1981). However, in the moats, it is likely that diffusion-limitation in microbial mats is the main factor creating carbon isotopic differences with depth. As discussed previously by Doran et al. (1998), photosynthetic rates are high during the 24-hour summer sunlight, creating a situation where DIC assimilation is controlled by the rate at which it diffuses into the mat, resulting in a reduced fractionation. This diffusion-limitation is typical of cyanobacterial assemblages and was also characterized by Schidlowski et al. (1984) and DesMarais (1989) in microbial mats of warm hypersaline environments.

In TV moats, POM is ^{13}C depleted relative to BOM, though both benthic and pelagic primary producers grow in waters with the same $[CO_2]_{aq}$. Although the contribution of pelagic photoautotrophy versus detrital input to moat POM is not precisely known, the significant depletion of moat POM during flood year relative to non-flood years suggests that the POM is dominated by photoautotrophic contributions. In Lake Fryxell, moat POM samples collected during the flood year are more ^{13}C depleted than 87% of the moat POM samples from the previous non-flood year. Lake Hoare, ELB, and WLB moat POM samples also show an isotopic depletion during the flood season.

It has been shown that POM primarily composed of phytoplankton have a wide range of $\delta^{13}C$, from −44 to −20‰ (e.g., Goericke et al., 1994; Goering et al., 1990), a range similar to that of $\delta^{13}C_{POM}$ found in the TV lakes. The fractionation of ^{13}C by phytoplankton is primarily controlled by the concentration of ambient $[CO_2]_{(aq)}$ (e.g., Degens et al., 1968; Fogel et al., 1992; Freeman and Hayes, 1992; Rau et al., 1996) and growth rate (Bidigare, 1997; Laws et al., 1995). Neumann et al. (1998, 2001) have demonstrated in Lakes Hoare and Fryxell that an increase in $[CO_2]_{(aq)}$ during summer glacial-melt, with the addition of stream derived CO_2 to the lakes accounts for greater

fractionation of carbon isotopes of DIC. Phytoplankton generally have higher specific growth rates than benthic mats (Goericke et al., 1994), therefore, making differences in growth rate unaccountable for the isotopic difference between moat POM and BOM. Fractionation between DIC and organic carbon also depends on cell wall permeability, cell size and geometry, as well as the ability of an organism to assimilate inorganic carbon (passively versus actively) (Goericke et al., 1994; Popp et al., 1998; Raven and Johnston, 1991). Thus, moat mats are enriched in ^{13}C relative to phytoplankton, because they must contend with the controlling effect of mucilage (a protective polysaccharide coating) and a colonial morphology, both of which limit the diffusion of CO_2 to assimilation sites (Des Marais and Canfield, 1994; Schidlowski et al., 1984).

During flood years, waters in the moat are well-mixed and very turbid, thereby we speculate that, in addition to the effects of higher concentration of dissolved CO_2 resulting from larger surface area for CO_2 exchange at the water-atmosphere boundary, reduced light penetration limits phytoplanktonic growth, resulting in greater ^{13}C fractionation and more depleted OM in the moats. These same hypotheses may be applied to explain depleted BOM samples during the flood year.

5.2. CARBON ISOTOPE PROFILES BELOW THE ICE-COVER

5.2.1. Influence of Flood Year

The isotopic differences observed in the moats between the flood and non-flood years are not observed below the ice-cover (Figure 7). SCUBA-observations detected only minor sedimentation increases under the ice in Lake Hoare following the flood year (I. Hawes, personal communication). Furthermore, BOM samples collected during all three seasons at similar depths are isotopically similar. These under-ice isotopic patterns are in agreement with previously published $\delta^{13}C_{BOM}$ and $\delta^{13}C_{DIC}$ profiles for Lake Hoare (Doran et al., 1998; Neumann et al., 1998; Wharton et al., 1993). The $\delta^{13}C_{DIC}$ profiles for Lake Fryxell, WLB, and ELB are also in close agreement with those from 1994–1995 and 1996–1997 seasons, showing with depth the depletion of $\delta^{13}C_{DIC}$ in Lake Fryxell and a large enrichment of ^{13}C in ELB (Neumann et al., 1998, 2004). However, our invariant WLB $\delta^{13}C_{DIC}$ profile does not show a $\sim 5‰$ enrichment in ^{13}C near the chemocline depth as reported by Neumann et al. (2004)

This constancy, combined with the stability of the water column below the ice in each of the lakes, implies that the moats and lake waters below the ice-cover can be considered as relatively isolated systems, in terms of water exchange and sediment transport, with only minor communication between

the two. This allows comparisons between POM, BOM, and DIC from three different years, independent of flood status.

However, we did test the influence of stream meltwater input on the isotopic composition of POM below the ice-cover (Figure 7). The only response we observe is amongst samples at 6 m depth where stream-proximal samples are systematically enriched in ^{13}C (3.5–5‰) relative to samples collected in the center of the basin, except in WLB, where the POM is invariant across the water column. Turbulent mixing in the open moat waters transfers to horizontal motions under the ice-cover, with minimal vertical mixing (Spigel and Priscu, 1998). At 6 m, $\delta^{13}C_{POM}$ values in stream-proximal areas trend toward those of the moat $\delta^{13}C_{POM}$ values. Thus, we propose that during years of large moat formation, the vertical/turbulent mixing can extend to at least 6 m depth in localities near moats that have been influenced by streams. This confirms the observation of Spigel and Priscu (1998) who showed that conductivity and temperature profiles at Lake Fryxell and ELB are influenced by melt water during higher flow years between 5 and 6 m.

5.2.2. $\delta^{13}C$ trends at the Chemocline

The water column above 11 m in Lake Fryxell supports active photosynthetic assemblages (Priscu, 1989, 1995; Vincent, 1981). The zone between 9 and 11 m is anoxic and photosynthesis is dominated by photosynthetic purple bacteria (Priscu et al., 1987a, b). The anoxic waters result from vertical transport and decay of POM (Neumann et al., 1998, 2001).

However, Doran et al. (1999) measured a 10,200–13,500 yr. ^{14}C age for POM and 1600–2,700 yr. ^{14}C age for the DIC of Lake Hoare. These ages indicate that the under-ice POM includes some ancient carbon, though the exact proportion of ancient, recycled material is currently unknown.

The negative excursion (3–4‰ depletion between 8 and 9.5 m depth) in the POM profile just above the chemocline (Figure 7a) may result from a variety of processes: (i) respiration by heterotrophs of ^{13}C depleted CO_2 and the subsequent use of this ^{13}C depleted carbon by photosynthetic primary producers living just above the chemocline; (ii) stronger discrimination against ^{13}C from the biota at 8–9.5 m depth; (iii) lateral mixing during high stream flows and high wind events in the moat waters create enriched $\delta^{13}C_{POM}$ at 6 m depth (positive shift), creating the appearance of a negative excursion below 6 m; (iv) diffusion of ^{13}C depleted DIC from below the chemocline. This last process can be discounted, as the DIC just below the chemocline is not significantly depleted in ^{13}C relative to DIC above the chemocline. The effect of wind-driven mixing seems to be limited to stream-proximal and other areas located near moats. Because the negative excursion above the chemocline is also observed in stream-distal profiles away from moats, it is unlikely

the product of stream and moat influences. Thus, we are left with processes (i) and (ii) and the latter cannot be addressed at this time due to lack of knowledge of the biota living just above the chemocline. Process (i) is supported by the fact that aerobic respiration is the dominant pathway of OM degradation, and consistent with the density stratified water column and an apparent absence of pellet-forming grazers, as decomposing POM is, in part, maintained in the water column (Howes and Schlezinger, 1992). Neumann et al. (1998, 2001), through investigating concentrations and the isotopic composition of DIC, also indicate OM mineralization at depth as a significant contribution to the carbon cycle of Lake Fryxell.

At its chemocline, East Lake Bonney shows a response in $\delta^{13}C_{POM}$ opposite to that in Lake Fryxell. Between 15 and 20 m, there is a 3–4‰ enrichment in $^{13}C_{POM}$, and subsequent 1–2‰ depletion below the chemocline (Figure 7). This enrichment may be due to a large utilization by POM source organisms of DIC that enter the trophogenic zone via upward diffusion across the chemocline (Priscu et al., 1999). Priscu et al. (1996) and Voytek et al. (1999) have concluded that there is chemotrophic fixation of CO_2 by aerobic ammonia oxidizing bacteria above the ELB chemocline. The DIC below the chemocline is likely a remnant carbon pool, a ''legacy'' from a previous evapoconcentration climatic event. The presence of photosynthetic sulfur oxidizing bacteria that discriminate less against ^{13}C than cyanobacteria during CO_2 uptake (e.g., Preuss et al., 1989), could also explain such a positive trend at the chemocline, as light does penetrate into the anoxic zone (Figure 3a) making anoxygenic photoautotrophy possible. However, there are no reports in ELB of the presence of hydrogen sulfide, a typical proton donor for anoxygenic phototrophic bacteria, and calculated Gibb's free energies (Lee et al., 2004) would not support the necessary reactions. Moreover, there is no biological evidence in support of the presence of sulfide oxidizing bacteria in ELB. Stable isotopic signatures below the chemocline do not indicate decomposition of POM, as there is not a significant negative shift in the DIC profile with depth. Priscu (1992), using $^{14}CO_2$ release from ^{14}C-labelled glucose, determined very little decomposition below the trophogenic zone in a region where heterotrophic bacterial production measured by tritiated thymidine incorporation was negligible, despite high cell densities ($\sim 10^5$ cells ml^{-1}). The presence of very low bacterial activities was again confirmed in a more recent study by Ward et al. (2003). As a result, this positive excursion in $\delta^{13}C_{POM}$ cannot be explained at this point.

5.2.3. $\delta^{13}C$ at Maximum Depths

In ELB, WLB, Lake Hoare, and Lake Fryxell, $\delta^{13}C_{POM}$ and $\delta^{13}C_{BOM}$ at maximum depths are the same. The similarity in the $\delta^{13}C_{POM}$ and $\delta^{13}C_{BOM}$

values suggests that in all lakes the deepest BOM has the largest contribution from the particulate component. However, our data indicate that BOM and POM components in Lake Fryxell and Lake Hoare are mostly independent, while in ELB and WLB, the BOM and POM seem closely related. The relative proportion of benthic primary productivity to total lake productivity can explain this difference.

Lake Fryxell and Lake Hoare have large basin-wide benthic contributions to total lake metabolism (Hawes and Schwarz, 1999; Priscu et al., 1995). Wharton et al. (1993) suggested that carbon fixed in the euphotic zone of Lake Hoare is rapidly mineralized in the water column or at the sediment/water interface, with net losses of nitrogen as compared to carbon. This suggests that pelagic primary produced POM represents a small component of the accumulated OM on the shallow slopes of the lake basin relative to BOM, consistent with differences between $\delta^{13}C_{POM}$ and $\delta^{13}C_{BOM}$ at shallower depths. At maximum depth, where benthic primary productivity is likely less than on the slopes, the pelagic primary produced POM dominates the accumulated organic matter, consistent with the equal $\delta^{13}C_{POM}$ and $\delta^{13}C_{BOM}$ at maximum depths.

WLB $\delta^{13}C_{POM}$ transects and $\delta^{13}C_{BOM}$ are the same values and invariant with depth, suggesting that the bulk BOM reflects the POM throughout the water column. This same relationship may be true for ELB where the only difference between $\delta^{13}C_{BOM}$ and $\delta^{13}C_{POM}$ is at 6 m depth (Figure 7d). As described previously, ELB and WLB are extremely steep-sided, which likely favors planktonic over benthic productivity in the lakes, as steep basin slopes provide a lesser area of illuminated habitat for microbial mat growth. Priscu et al. (1999) modeled the pelagic food web and associated carbon fluxes for ELB, showing sediment flux is comprised of both material settling from the water column and ice-cover. The pelagic component comprises the largest of the modeled depth-integrated carbon flux (8556 mg m^{-2} yr^{-1}) to the buried carbon at the lake bottom (Priscu et al., 1999). The dominance of pelagic primary productivity over benthic primary productivity explains the similarity between $\delta^{13}C$ of POM and BOM, below the chemocline in ELB and WLB.

5.2.4. $\delta^{13}C$ of Sediment Trap Organic Matter

The weighted carbon isotopic signature for ELB total trapped sediment has a $\delta^{13}C$ ($-13.9 \pm 0.7‰$) not significantly different from those observed for the mean $\delta^{13}C$ of >250 μm grain size fraction ($-13.9 \pm 2.6‰$) and ELB moat BOM ($-13.6 \pm 3.9‰$). In contrast, the weighted carbon isotopic signature of WLB trapped sediments ($-30.5 \pm 0.5‰$) is not significantly different from that of the <63 μm grain size fraction ($-31.1 \pm 0.7‰$) as well as those of ELB BOM and POM below 6 m. ELB trapped sediments are dominated by

the largest grain size fraction, which contains the bulk of the particulate fallout organic carbon (78.4%, n = 13). The intermediate particle size (63–250μm) represents 20.1% (n = 13) of the organic carbon fallout. In contrast, WLB trapped sediments are dominated by the finest grain size fraction (<63 μm), which also represents the bulk of the organic carbon fallout (97.7%, n = 14). The >250 μm grains size fraction provides the next largest influx of carbon (1.8% n = 14), while the intermediate grain size fraction (63–250 μm) is the least (0.5%, n = 14).

Surface water circulation in Lake Bonney typically follows a west–east flow path owing to higher hydraulic inputs in WLB (J. Priscu, unpublished data). It has also been shown that weak turbulent mixing occurs along the sides and bottoms of the shallow, narrow passage connecting ELB and WLB (Spigel and Priscu, 1998). It can be hypothesized that this turbulence may be responsible for the inputs of "moat-like" OM into the sediment traps in ELB. However, the distance between the sediment trap in ELB and the narrow channel between WLB and ELB ($\sim$3 km) make that hypothesis improbable. The most plausible hypothesis for the difference between $\delta^{13}C_{BOM}$ and $\delta^{13}C_{trap}$ in ELB is the contribution of sediments and OM released from the ice-cover in an episodic so-called "sediment dump" event (Nedell et al., 1987; Simmons et al., 1986; Wharton et al., 1989). In support of that hypothesis, the average $\delta^{13}C$ values of OM in the ice-cover sediments measured at Lake Hoare ($-14.4 \pm 3.0‰$, n = 3) are not significantly different from the weighted $\delta^{13}C$ average calculated for ELB trapped sediments ($-13.9 \pm 0.7‰$).

Lake Hoare sediment traps (placed at 8 m depth) have similar carbon isotopic signatures as POM collected at 5.5 m in the stream proximal profile. The POM at this site is enriched in ^{13}C relative to POM from the deep profile, indicating that waters in shallow under-ice settings may receive contribution from moat organic matter. However, none of the 10 sediment traps at this depth caught a sediment dump event from the overlying ice-cover, as sediments were all finer than <63 μm.

6. Conclusions

In the four TV lakes studied, moat and under-ice OM have distinctly different carbon isotope compositions, with moat OM being significantly enriched in ^{13}C relative to OM of deeper environments. There is a sharp $\delta^{13}C$ value boundary at $-20‰$ for BOM and at $-26‰$ for POM separating these two environments. In contrast, this distinction is not observed in the $\delta^{15}N$ values, with both moat and under-ice OM spanning a relatively narrow range. Thus, $\delta^{13}C$ of OM can be a proxy for sample position in the lake in paleolimnological reconstruction of perennially ice-covered lakes.

In the moat, the carbon isotopic composition of BOM is not apparently influenced by the composition of cyanobacterial assemblages. The main factor influencing the isotopic composition of moat BOM is the CO_2 diffusion-limitation across cell membranes associated with the polysaccharide sheath and colonial nature of cyanobacterial assemblages. Moat POM, mostly phytoplanktonic, is significantly depleted in ^{13}C relative to BOM. During a year of enhanced glacial melt and formation of wide moats, we observed that both $\delta^{13}C_{POM}$ and $\delta^{13}C_{BOM}$ signatures become more negative by 5–15‰ relative to non-flood years. We hypothesize that this trend in the moats might be the result of a reduced growth rate of photoautotrophic primary producers in the moat, in response to turbidity-induced light limitation and/or increased $[CO_2]_{(aq)}$.

In the under-ice environment, at a depth of 6 m, the more positive values of $\delta^{13}C_{POM}$ in stream-proximal sites relative to deep-profiles sites suggest that lateral mixing of moat waters extends to at least 6 m in areas situated near large moats or stream inputs.

In all lakes, the $\delta^{13}C_{POM}$ and $\delta^{13}C_{BOM}$ signatures at maximum depths are similar. This similarity suggests that the BOM in the deepest areas of the lakes receive the largest contribution from POM. However, at shallower depths, our data indicate that the BOM and POM systems in Lake Fryxell and Lake Hoare are mostly unconnected, with BOM being more enriched in ^{13}C relative to the POM, demonstrating the greater influence of benthic primary productivity in those two lakes. In contrast, in ELB and WLB, the $\delta^{13}C_{POM}$ and $\delta^{13}C_{BOM}$ seem closely related throughout the water column, suggesting the dominance of the pelagic (POM) component in the carbon cycle of these lakes. This is further supported by the sediment trap data for WLB, which indicate that the water column fallout is dominated by fine (< 63 μm) particles with a weighted carbon isotopic composition (-30.5 ± 0.5‰) similar to those of POM and BOM.

In contrast, sediment trap data for ELB record a water column fallout dominated by the largest grain size fraction (> 250 μm) with a weighted isotopic composition (-13.9 ± 0.7‰) similar to that of lake ice sediments, but completely different from BOM and POM. These sediments were likely released from the ice-cover during an episodic sediment dump event.

The processes responsible for the stable carbon isotopic excursions observed at the chemoclines of Lake Fryxell and ELB are unclear at this time. The chemoclines are spatially limited environments with extreme physiochemical properties, unique to each lake. Moreover, our knowledge of the organisms present at the chemocline, though increasing (e.g., Karr et al., 2003), is still limited. Thus, further biological investigation and compound specific isotope analyses might be needed before these POM profiles can be fully understood.

Acknowledgements

This work is supported by NSF Long Term Ecological Research program and Office of Polar Programs (OPP 9810219, OPP 0096259) and the NASA Exobiology Program (NAG5-9427). We thank Chris Fritsen and Sarah Marshall who performed microbial mat species identification. We would also like to thank Linnea Heraty and Lora Wingate for analytical support. We thank Ian Hawes for discussions about benthic productivity and assistance with sample collection. Field help was provided by Richard Costello, Christine Foreman, Derek Mueller, Carrie Olsen, Maria Uhle, and Craig Wolf. Raytheon Polar Services and Petroleum Helicopters Inc., provided logistical services in the field.

References

Adams E. E., Priscu J. C., Fritsen C. H., Smith S. R. and Brackman S. L. (1998) Permanent ice covers of the McMurdo dry valley lakes, Antarctica; bubble formation and metamorphism. In *Ecosystem Dynamics in a Polar Desert; the McMurdo Dry Valleys, Antarctica*, Vol. 72 (ed. J. C. Priscu), pp. 281–295. American Geophysical Union.

Andersen D. T., McKay C. P. and Wharton R. A. (1998) Dissolved gases in perennially ice-covered lakes of the McMurdo dry valleys, Antarctica. ***Antarctic Sci.*** **10**(2), 124–133.

Andersen D. W., Wharton R. A. J. and Squyres S. W. (1993) Terrigenous clastic sedimentation. In *Physical and Biogeochemical processes in Antarctic Dry Valley Lakes*, Vol. 59 (ed. E. I. Friedmann), pp. 71–81. American Geophysical Union.

Bernasconi S. M., Barbieri A., and Simona M. (1997) Carbon and nitrogen isotope variation in sedimenting organic matter in Lake Lugano. *Limnol. Oceanogr.* **42**(8), 1755–1765.

Bidigare R. R. (1997) Consistent fractionation of ^{13}C in nature and in the laboratory: Growth-rate effects in some haptophyte algae. *Global Biogeochem. Cycles* **11**, 279–292.

Bishop J. L., Lougear A., Newton J., Doran P. T., Froeschl H., Trautwein A. X., Korner W. and Koeberl C. (2001) Mineralogical and geochemical analyses of Antarctic lake sediments: A study of reflectance and Mossbauer spectroscopy and C, N, and S isotopes with applications for remote sensing on Mars. *Geochimica et Cosmochimica Acta*. **65**(17), 2875–2897.

Brenner M., Whitmore T., Curtis J. H, Hodell D. A., and CL S. (1999) Stable isotope (delta C-13 and delta N-15) signatures of sedimented organic matter as indicators of historic lake trophic state. *J. Paleolimnol.* **22**(2), 205–221.

Burkins M. B., Virginia R. A., Chamberlain C. P. and Wall D. H. (2000) Origin and distribution of soil organic matter in Taylor Valley, Antarctica. *Ecol.* **81**(9), 2377–2391.

Degens E. T., Guillard R. R. L., Sackett W. M. and Helleburst J. A. (1968) Metabolic fractionation of carbon isotopes in marine plankton: Temperature and respiration experiments. *Deep-Sea Res.* **15**, 1–9.

Des Marais D. J. and Canfield D. E. (1994) The carbon isotope biogeochemistry of microbial mats. In *Microbial Mats: Structure, Development, and Environmental Significance* (Ed. P. Caumette), pp. 289–298. Springer-Verlag.

Des Marais D. J., Cohen Y., Nguyen H., Cheatham T. and Munoz E. (1989) Carbon isotopic trends in the hypersaline ponds and microbial mats at Guerrero Negro, Baja California Sur, Mexico: Implications for Precambrian stromatolites. In *Microbial Mats: Physiological Ecology of Benthic Microbial Communities* (ed. E. Rosenberg), pp. 191–205. American Society for Microbiology.

Doran P. T., Berger G. W., Lyons W. B., Wharton R. A., Davisson M. L., Southon J. and Dibb J. E. (1999) Dating Quaternary lacustrine sediments in the McMurdo Dry Valleys, Antarctica. *Palaeogeograph. Palaeoclimatol. Palaeoecol.* **147**(34), 223–239.

Doran P. T., McKay C. P., Clow G. D., Dana G. L., Fountain A. and Nylen T. (2002a) Valley floor climate observations from the McMurdo Dry Valleys, 1986–2000. *J. Geophys. Res. - Atmospheres* **107**(D24).

Doran P. T., Priscu J. C., Lyons W. B., Powell R., Andersen D. T. and Poreda R. (2004) Paleolimnology of extreme cold environments. In *Long-term environmental change in Arctic and Antarctic lakes*, in press, Kluwer Academic Press.

Doran P. T., Priscu J. C., Lyons W. B., Walsh J. E., Fountain A. G., McKnight D. M., Moorhead D. L., Virginia R. A., Wall D. H., Clow G. D., Fritsen C. H., McKay C. P. and Parsons A. N. (2002b) Antarctic climate cooling and terrestrial ecosystem response. *Nature* **415**(6871), 517–520.

Doran P. T., Wharton R. A., Des Marais D. J. and McKay C. P. (1998) Antarctic paleolake sediments and the search for extinct life on Mars. *J. Geophys Res.* **103**(E12), 28481–28493.

Fogel M. L., Cifuentas L. A., Velinsky D. J. and Sharp J. H. (1992) Relationship of carbon availability in estuarine phytoplankton to isotopic composition. *Marine Ecol.-Progress Series* **82**(3), 291–300.

Fountain A., Lyons W. B., Burkins M. B., Dana G. L., Doran P. T., Lewis K. J., McKnight D., Moorhead D. L., Parsons A. N., Priscu J. C., Wall D. H., Wharton R. A. J. and Virginia R. A. (1999) Physical controls on the Taylor Valley Ecosystem, Antarctica. *Bioscience* **49**(12), 961–972.

Freeman K. H. and Hayes J. M. (1992) Fractionation of carbon isotopes by phytoplankton and estimates of ancient CO_2 levels. *Global Biogeochem. Cycles* **6**, 627–644.

Fritsen C. H., Grue A. M. and Priscu J. C. (2000) Distribution of organic carbon and nitrogen in surface soils in the McMurdo Dry Valleys, Antarctica. *Polar Biol.* **23**(2), 121–128.

Fuchs G. and Stupperich E. (1985) Evolution of CO_2 fixation. In *Evolution of Prokaryotes*, Vol. FEMS Symposium 29 (ed. S. E. Schleier), pp. 756–251. Academic Press.

Goericke R., Montoya J. P. and Fry B. (1994) Physiology of isotopic fractionation in algae and cyanobacteria. In *Stable Isotopes in Ecology and Environmental Science* (Ed. R. H. Michener), pp. 187–221. Blackwell Scientific Publications.

Goering J., Alexander V. and Haubenstock N. (1990) Seasonal variability of stable carbon and nitrogen isotope ratios of organisms in a North Pacific bay. *Estuarine Coastal Shelf Sci.* **30**(3), 239–269.

Gu B., Schelske C. L. and Brenner M. (1996) Relationship between sediment and plankton isotope ratios ($\delta^{13}C$ and $\delta^{15}N$) and primary productivity in Florida lakes. *Can. J. of Fish. Aqua. Sci.* **53**, 875–883.

Hall B. L. and Denton G. H. (2000a) Extent and chronology of the Ross Sea drift and the Wilson Piedmont Glacier along the Scott Coast at and since the last glacial maximum. *Geografiska Annaler Series A-Phys. Geogr.* **82A**(23), 337–363.

Hall B. L. and Denton G. H. (2000b) Radiocarbon chronology of Ross Sea drift, eastern Taylor Valley, Antarctica: Evidence for a grounded ice sheet in the Ross Sea at the last glacial maximum. *Geografiska Annaler Series A-Phys. Geogr.* **82A**(23), 305–336.

Hall B. L., Denton G. H. and Hendy C. H. (2000) Evidence from Taylor Valley for a grounded ice sheet in the Ross Sea, Antarctica. *Geografiska Annaler Series A-Phys. Geogr.* **82A**(23), 275–303.

Hamilton S. K. and Lewis W. M. J. (1992) Stable carbon and nitrogen isotopes in algae and detritus from the Orinoco river floodplain, Venezuela. *Geochimica et Cosmochimica Acta.* **56**(12), 4237–4246.

Harvey H. R., Tuttle J. H. and Bell J. T. (1995) Kinetics of phytoplankton decay during simulated sedimentation: Changes in biochemical composition and microbial activity under oxic and anoxic conditions. *Geochimica et Cosmochimica Acta*. **59**(16), 3367–3377.

Hawes I. and Schwarz A.-M. (1999) Photosynthesis in an extreme shade environment: Benthic microbial mats from Lake Hoare, a permanently ice-covered Antarctic lake. *J. Phycol*. **35**, 448–459.

Hecky R. E., Campbell P. and Hendzel L. L. (1993) The stoichiometry of carbon, nitrogen, and phosphorous in particulate matter of lakes and oceans. *Limnol. Oceanogr*. **38**, 709–724.

Hedges J. I., Baldock J. A., Yves G., Lee C., Peterson M. and Wakeham S. G. (2001) Evidence for non-selective preservation of organic matter in sinking marine particles. *Nature* **409**, 801–803.

Hendy C. H. (2000a) Late Quaternary lakes in the McMurdo Sound region of Antarctica. *Geografiska Annaler Series A-Phys. Geogr*. **82A**(23), 411–432.

Hendy C. H. (2000b) The role of polar lake ice as a filter for glacial lacustrine sediments. *Geografiska Annaler Series A-Phys. Geogr*. **82A**(23), 271–274.

Henrichs S. M. and Doyle A. P. (1986) Decomposition of ^{14}C-labeled organic substances in marine sediments. *Limnol. Oceanogr*. **319**(4), 765–778.

Howes B. L. and Schlezinger D. R. (1992) Carbon cycling in a redox-stratified Antarctic lake, Lake Fryxell. *Antarctic J. US*. **27**(5), 263–265.

Karr E. A., Sattley W. M., Jung D. O., Madigan M. T. and Achenbach L. A. (2003) Remarkable diversity of phototrophic purple bacteria in a permanently frozen Antarctic lake. *Appl. Environ. Microbiol*. **69**(8), 4910–1914.

Kendall C., Silva S. R. and Kelly V. J. (2001) Carbon and nitrogen isotopic compositions of particulate organic matter in four large river systems across the United States. *Hydrological Processes* **15**, 1301–1346.

Konley S. T. (2002) *Linkages Between Soils and Lake Ice Sediment Biogeochemistry: Taylor Valley, Southern Victoria Land Antarctica*. M.S. Thesis, Montana State University at Bozeman.

Laws E. A., Popp B. N., Bidigare R. R., Kennicutt M. C. and Macko S. A. (1995) Dependence of phytoplankton carbon isotopic composition on growth rate and $[CO_2]_{aq}$: Theoretical considerations and experimental results. *Geochimica et Cosmochimica Acta*. **59**(6), 1131–1138.

LaZerte B. D. (1983) Stable carbon isotope ratios: implications for the source sediment carbon and phytoplankton carbon assimilation in Lake Memphremagog, Quebec. *Can. J. Fish. Aqua. Sci*. **40**, 1658–1666.

Lee P. A., Mikucki J. A., Foreman C. M., Priscu J. C., DiTullio G. R., Riseman S. F. and de Mora S. J. (2004) Thermodynamic constraints on microbially mediated processes in lakes of the McMurdo Dry Valleys, Antarctica. *Geomicrobiol. J*. **21**(3), 221–237.

Lehmann M. F., Bernasconi S. M., Barbieri A. and McKenzie J. A. (2002) Preservation of organic matter and alteration of its carbon and nitrogen isotope composition during simulated and in situ early sedimentary diagenesis. *Geochimica et Cosmochimica Acta*. **66**(20), 3573–3584.

Lyons W. B., Frape S. K. and Welch K. A. (1999) History of McMurdo Dry Valley lakes, Antarctica, from stable chlorine isotope data. *Geology* **27**(6), 527–530.

Lyons W. B., Tyler S. W., Wharton R. A., McKnight D. M. and Vaughn B. H. (1998) A Late Holocene desiccation of Lake Hoare and Lake Fryxell, McMurdo Dry Valleys, Antarctica. *Antarctic Sci*. **10**(3), 247–256.

Macko S. A. and Ostrom N. E. (1994) Molecular and pollutions studies using stable isotopes. In *Stable Isotopes in Ecology and Environmental Science*, Vol. 5–62 (Ed. R. H. Michener), p. 4. Blackwell Scientific Publications.

McKay C. P., Clow G., Wharton Jr. R. A. and Squyres S. W. (1985) Thickness of ice on perennially frozen lakes. *Nature* **313**, 561–562.

McKenzie J. A. (1980) Carbon-13 cycle in Lake Greifen: A Model for restricted ocean basins. In *Nature and Origin of Cretaceous carbon-rich facies* (ed. S. O. Schlanger), pp. 197–207.

McKnight D. M. and Andrews E. D. (1993a) Hydrologic and geochemical processes at the stream-lake interface in a permanently ice-covered lake in the McMurdo Dry Valleys, Antarctica. *Verhandlungen-Internationale Vereinigung fuer Theoretische und Angewandte Limnologie* **25**(2), 957–959.

McKnight D. M. and Andrews E. D. (1993b) Potential hydrologic and geochemical consequences of the 1992 merging of lake Chad with Lake Hoare in Taylor Valley. *Antarctic J.-review*, 249–251.

Meyers P. A. and Eadie B. J. (1993) Sources, degradation and recycling of organic matter associated with sinking particles in Lake Michigan. *Organic Geochem* **20**(1), 47–56.

Meyers P. A. and Ishiwatari R. (1993) Lacustrine organic geochemistry—an overview of indicators of organic matter sources and diagenesis in lake sediments. *Organic Geochem.* **20**(7), 867–900.

Miller L. G. and Aiken G. R. (1996) Effects of glacial meltwater inflows and moat freezing on mixing in an ice-covered Antarctic lake as interpreted from stable isotope and tritium distributions. *Limnol. Oceanogr.* **41**(5), 966–976.

Nedell S. S., Andersen D. W., Squyres S. W. and Love F. G. (1987) Sedimentation in ice-covered Lake Hoare, Antarctica. *Sedimentology* **34**, 1093–1106.

Neumann K., Lyons W. B. and Des Marais D. J. (1998) Inorganic carbon-isotope distribution and budget in the Lake Hoare and Lake Fryxell basins, Taylor Valley, Antarctica. *Annals Glaciol* **27**, 685–689.

Neumann K., Lyons W. B., Priscu J. C., Des Marais D. J. and Welch K. A. (2004) The carbon isotopic composition of dissolved inorganic carbon in perennially ice-covered antarctic lakes: Searching for a biogenic signature. *Annals of Glaciol.* in press.

Neumann K., Lyons W. B., Priscu J. C. and Donahue R. J. (2001) CO_2 concentrations in perennially ice-covered lakes of Taylor Valley, Antarctica. *Biogeochemistry* **56**, 27–50.

O'Leary M. H. (1981) Carbon isotope fractionation in plants. *Phytochemistry* **20**, 553–567.

Ostrom N. E., Long D. T., Bell E. M. and Beals T. (1998) The origin and cycling of particulate and sedimentary organic matter and nitrate in Lake Superior. *Chem. Geol.* **152**(12), 13–28.

Popp B. N., Laws E. A., Bidigare R. R., Dore J. R., Hanson K. L. and Wakeham S. G. (1998) Effect of phytoplankton cell geometry on carbon isotope fractionation. *Geochimica et Cosmochimica Acta* **62**(1), 69–77.

Preuss A., Schauder R. and Fuchs G. (1989) Carbon isotope fractionation by autotrophic bacteria with three different CO_2 fixation pathways. *Zeitschrift fur Naturforschung* **44 C**, 397–402.

Priscu J. C. (1989) Photon dependence of inorganic nitrogen transport by phytoplankton in perennially ice-covered Antarctic lakes. *Hydrobiologia* **172**, 173–182.

Priscu J. C. (1992) Particulate organic matter decomposition in the water column of Lake Bonney, Taylor Valley, Antarctica. *Antarctic J. US.* **27**(5), 260–262.

Priscu J. C. (1995) Phytoplankton nutrient deficiency in lakes of the McMurdo Dry Valleys, Antarctica. *Freshwater Biol.* **34**(2), 215–227.

Priscu J. C. (1998) Ecosystem dynamics in a polar desert; the McMurdo dry valleys, Antarctica. In *Antarctic Research Series*, Vol. 72, p. 369. American Geophysical Union.

Priscu J. C., Downes M. T. and McKay C. P. (1996) Extreme supersaturation of nitrous oxide in a poorly ventilated Antarctic lake. *Limnol. Oceanogr.* **41**(7), 1544–1551.

Priscu J. C., Fritsen C. H., Adams E. E., Giovannoni S. J., Paerl H. W., McKay C. P., Doran P. T., Gordon D. A., Lanoil B. D. and Pinckney J. L. (1998) Perennial Antarctic lake ice: An oasis for life in a polar desert. *Science* **280**(5372), 2095–2098.

Priscu J. C., Priscu L. R., Howard-Williams C. and Vincent W. F. (1987a) Photosynthate biosynthesis by phytoplankton in permanently ice-covered Antarctic lakes under continuous sunlight. *J. Plankton Res.* **10**(1), 333–340.

Priscu J. C., Priscu L. R., Vincent W. F. and Howard-Williams C. (1987b) Photosynthate distribution by microplankton in permanently ice-covered Antarctic desert lakes. *Limnol. Oceanogr.* **2**(1), 260–270.

Priscu J. C., Wolf C. F., Takacs C. D., Fritsen C. H., Laybourn-Parry J., Roberts E. C., Sattler B. and Lyons W. B. (1999) Carbon transformations in a perennially ice-covered Antarctic lake. *Bioscience* **49**(12), 997–1008.

Quay P. D., Emerson S. R., Quay B. M. and Devol A. H. (1986) The carbon cycle for Lake Washington - A stable isotope study. *Limnol. Oceanogr.* **31**, 596–611.

Quay P. D., Wilbur D. O., Richey J. E., Hedges J. I. and Devol A. H. (1992) Carbon cycling in the Amazon River: implications from the ^{13}C compositions of particles and solutes. *Limnol. Oceanogr.* **37**, 857–871.

Rau G. H., Riebesell U. and Wolf-Gladrow D. (1996) A model of photosynthetic ^{13}C fractionation by marine phytoplankton based on diffusive molecular CO_2 uptake. *Marine Ecology-Progress Series* **133**, 275–285.

Raven J. A. and Johnston A. M. (1991) Mechanisms of inorganic-carbon acquisition in marine phytoplankton and their implications for the use of other resources. *Limnol. Oceanogr.* **36**, 1701–1714.

Schidlowski M., Matzigkeit U. and Krumbein W. E. (1984) Superheavy organic carbon from hypersaline microbial mats. *Naturwissenschaften* **71**, 303–308.

Simmons G. M., Jr., Wharton R. A., Jr., McKay C. P., Nedell S. and Clow G. (1986) Sand/ice interactions and sediment deposition in perennially ice-covered Antarctic lakes. *Antarctic J. US.* **21**, 217–220.

Spigel R. H. and Priscu J. C. (1998) Physical limnology of the McMurdo Dry Valley lakes. In *Ecosystem Dynamics in a Polar Desert: The McMurdo Dry Valleys, Antarctica*, Vol. 72 (Ed. J. C. Priscu), pp. 153–187. American Geophysical Union.

Tyler S. W., Cook P. G., Butt A. Z., Thomas J. M., Doran P. T. and Lyons W. B. (1998) Evidence of deep circulation in two perennially ice-covered Antarctic lakes. *Limnol. Oceanogr.* **43**(4), 625–635.

Vincent W. F. (1981) Production strategies in Antarctic inland waters: Phytoplankton ecophysiology in a permanently ice-covered lake. **62**(5), 1215–1224.

Voytek M. A., Priscu J. C., and Ward B. B. (1999) The distribution and relative abundance of ammonia-oxidizing bacteria in lakes of the McMurdo Dry Valley, Antarctica. *Hydrobiologia* **401**, 113–130.

Ward B. B., Granger J., Maldonado M. T. and Wells M. L. (2003) What limits bacterial production in the suboxic region of permanently ice-covered Lake Bonney, Antarctica? *Aquatic Microbial. Ecol.* **31**(1), 33–47.

Wharton R. A., Jr., Lyons W. B. and Des Marais D. J. (1993) Stable isotopic biogeochemistry of carbon and nitrogen in a perennially ice-covered Antarctic lake. *Chem. Geol.* **107**(12), 159–172.

Wharton R. A., Jr., McKay C. P., Parker B. C. and Simmons G. M., Jr. (1986) Oxygen budget of a perennially ice-covered Antarctic dry valley lake. *Limnol. Oceanogr.* **31**, 437–443.

Wharton R. A., Jr., Parker B. C. and Simmons G. M., Jr. (1983) Distribution, species composition and morphology of algal mats in Antarctic dry valley lakes. *Phycologia* **22**(4), 355–365.

Wharton R. A., McKay C. P., Mancinelli R. L. and Simmons G. M. (1987) Perennial N_2 Supersaturation in an Antarctic Lake. *Nature* **325**(6102), 343–345.

Wharton R. A. J., Simmons G. M. J. and McKay C. P. (1989) Perennially ice-covered Lake Hoare, Antarctica: physical environment, biology and sedimentation. *Hydrobiologia* **172**, 305–320.